



Published in final edited form as:

Nanomedicine. 2017 February ; 13(2): 443–454. doi:10.1016/j.nano.2016.07.015.

A nanoparticle-based nicotine vaccine and the influence of particle size on its immunogenicity and efficacy

Zongmin Zhao^{a,*}, Yun Hu^{a,*}, Reece Hoerle^a, Meaghan Devine^a, Michael Raleigh^b, Paul Pentel^b, and Chenming Zhang^{a,†}

^aDepartment of Biological Systems Engineering, Virginia Tech, Blacksburg, VA 24061, United States

^bMinneapolis Medical Research Foundation, Minneapolis, MN 55404, United States

Abstract

Traditional hapten-protein conjugate nicotine vaccines have shown less than desired immunological efficacy due to their poor recognition and internalization by immune cells. We developed a novel lipid-polymeric hybrid nanoparticle-based nicotine vaccine to enhance the immunogenicity of the conjugate vaccine, and studied the influence of particle size on its immunogenicity and pharmacokinetic efficacy. The results demonstrated that the nanovaccines, regardless of size, could induce a significantly stronger immune response against nicotine compared to the conjugate vaccine. Particularly, a significantly higher anti-nicotine antibody titer was achieved by the 100 compared to the 500 nm nanovaccine. In addition, both the 100 and 500 nm nanovaccines reduced the distribution of nicotine into the brain significantly. The 100 nm nanovaccine exhibited better pharmacokinetic efficacy than the 500 nm nanovaccine in the presence of alum adjuvant. These results suggest that a lipid-polymeric nanoparticle-based nicotine vaccine is a promising candidate to treat nicotine dependence.

Graphical Abstract

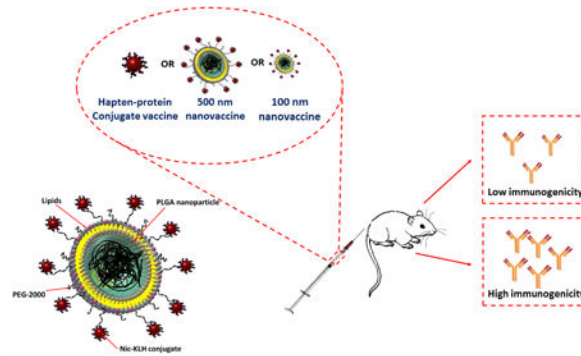
This work describes a novel strategy to enhance the immunogenicity of conjugate nicotine vaccines by using hybrid NPs as delivery vehicles. The work also suggests a method to improve the efficacy of NP-based nicotine vaccines by modulating the particle size. *In vivo* results indicate that a lipid-polymeric hybrid NP-based nicotine nanovaccine exhibits significantly higher immunogenicity than a conjugate nicotine vaccine, and that the 100 nm nanovaccine provided better immunogenicity and pharmacokinetic efficacy than the 500 nm nanovaccine. Overall, the findings suggest that a lipid-polymeric hybrid NP-based nicotine vaccine is a promising candidate to treat nicotine addiction.

[†]Correspondence to: Chenming (Mike) Zhang, Address: 210 Seitz Hall, Department of Biological Systems Engineering, Virginia Tech University, Blacksburg, VA 24061, USA, Voice: +1-(540)231-7601, Fax: +1-(540)231-3199, chzhang2@vt.edu.

^{*}These authors contributed equally to this work.

Potential conflict of interest: C.Z., Z.Z., and Y.H. have a related patent disclosure filed in December 2015 (VTIP disclosure 16-087). The other authors have no conflict of interest to disclose.

Publisher's Disclaimer: This is a PDF file of an unedited manuscript that has been accepted for publication. As a service to our customers we are providing this early version of the manuscript. The manuscript will undergo copyediting, typesetting, and review of the resulting proof before it is published in its final citable form. Please note that during the production process errors may be discovered which could affect the content, and all legal disclaimers that apply to the journal pertain.



Keywords

Nicotine addiction; nicotine vaccine; lipid-polymeric hybrid nanoparticle; anti-nicotine antibody; nanovaccine size

Background

Tobacco addiction has consistently been the top preventable cause of many serious diseases; it continues to result in extensive mortality, morbidity, and economic loss.^{1, 2} Currently, nicotine replacement therapies, bupropion, and varenicline, are the major pharmacological interventions available to smokers for quitting smoking.³ However, even with the help of these medications, the smoking cessation rate is disappointingly low (10-25%) and there are many associated problems, such as various adverse side effects and high cost.^{4, 5} Therefore, it is both necessary and urgent to develop new approaches to combat tobacco addiction.

In recent years, nicotine vaccines that can induce the production of nicotine-specific antibodies have emerged as a promising approach to combat smoking addiction.^{6, 7} The antibodies elicited by a nicotine vaccine can bind with nicotine molecules in blood to form antibody-nicotine complexes, thereby blocking nicotine from crossing the blood-brain barrier to stimulate the central nervous system.⁸ In the past decade, there have been several nicotine vaccine candidates developed and evaluated in human clinical trials.⁹ Unfortunately, none of these vaccines are currently available to smokers due to their poor efficacy caused by low antibody titers, high variability, and low antibody affinity for nicotine.⁷ The placebo-controlled phase 2 clinical studies of NicVax and NicQ β revealed that, while the overall smoking cessation rate was not enhanced compared to the placebo group, the top 30% of subjects that had the highest antibody titers showed an improved quit rate.^{10, 11} This suggests that the basic concept of immunotherapy for smoking cessation is solid but requires more antibodies to be generated to ensure efficacy of the vaccination.

To date, most existing nicotine vaccines are traditional hapten-protein conjugate vaccines in which nicotine analogues are conjugated to a carrier protein to be immunogenic.^{11, 12} However, traditional nicotine-protein conjugate vaccines suffer from several shortcomings, including poor recognition and internalization by immune cells, low bioavailability, fast degradation, difficulty in integration with molecular adjuvants, and short immune persistence, all of which lead to low immunological efficacy⁷.

Nanoparticles (NPs) have been extensively applied for efficient delivery of drugs, antigens, and vaccines,¹³⁻¹⁷ making them a promising approach to potentially overcome the limitations of conjugate nicotine vaccines. However, to our knowledge, the use of nanoparticles for the delivery of drug conjugate vaccines has not been widely studied, with only a few studies reporting the utilization of liposomes and negatively charged nanohorn-supported liposomes as nicotine vaccine delivery vehicles.¹⁸⁻²⁰ Nevertheless, liposomes and nanohorn-supported liposomes have either stability issues or safety concerns, limiting their clinical applications.

Lipid-polymeric hybrid NPs that consist of a poly(lactic-co-glycolic acid) (PLGA) NP core and a lipid shell, both of which have been approved for clinical use, have been used widely as vaccine delivery systems due to their biocompatibility, biodegradability, excellent safety, good stability, ease in fabrication, and ability in controlled antigen release.²¹⁻²³ In the current study, we developed a novel NP-based nicotine vaccine in which lipid-polymeric hybrid NPs were utilized as vehicles for the effective delivery of conjugate nicotine vaccines. Particularly, based on the hypothesis that NP size may affect the immunogenicity of NP-based nicotine vaccines, we determined whether the immunogenicity of nanovaccines could be enhanced by modulating NP size. In this study, we selected 100 and 500 nm as representatives of small and large sizes of lipid-polymeric NP-based nicotine vaccines. We compared the physicochemical properties, cellular uptake by dendritic cells, immunogenicity, pharmacokinetic (PK) efficacy, and safety of the nanovaccines with these two sizes.

Methods

Synthesis of a Nic-KLH conjugate

O-Succinyl-3'-hydroxymethyl-(±)-nicotine (Nic)-keyhole limpet hemocyanin (KLH) conjugates were synthesized using a carbodiimide-mediated reaction. In brief, 2.4 mg of Nic hapten were mixed with appropriate amounts of 1-ethyl-3-(3-dimethylaminopropyl)carbodiimide hydrochloride (EDC) and *N*-hydroxysulfosuccinimide (Sulfo-NHS) in 0.5 mL of activation buffer (0.1 M 2-(*N*-morpholino)ethanesulfonic acid, 0.5 M NaCl, pH 6.0), and incubated at room temperature for 15 min. The mixture was then added to 5 mg of KLH that was dissolved in 2 mL of coupling buffer (0.1 M sodium phosphate, 0.15 M NaCl, pH 7.2). After reacting overnight, unconjugated Nic hapten and byproducts were eliminated by dialyzing against 0.01 M phosphate-buffered saline (PBS) (pH 7.4) using a dialysis membrane (molecular weight cut-off 6000-8000) at room temperature for 24 h.

Assembly of lipid-polymeric hybrid NP-based nicotine vaccines

Lipid-polymeric hybrid NPs were assembled by attaching Nic-KLH conjugates onto the surface of lipid-PLGA hybrid NPs via a thiol-maleimide-mediated method. In brief, PLGA and lipid-PLGA NPs were fabricated according to the method described in the supplementary materials. An appropriate amount of Traut's reagent was added to 3 mg of Nic-KLH that was dissolved in 0.1 M pH 8.0 bicarbonate buffer, and incubated for 1 h at room temperature to obtain the thiolated Nic-KLH conjugate. Nic-KLH was attached onto

lipid-PLGA NPs by reacting the thiolated Nic-KLH with appropriate amounts of lipid-PLGA NPs in 0.1 M, pH 8.0, bicarbonate buffer for 2 h. Nanovaccine NPs were collected by centrifugation at 10,000 *g*, 4°C, for 30 min. Unattached Nic-KLH in the supernatant was quantified by the bicinchoninic acid assay.

Active immunization of mice with nicotine nanovaccines

All animal studies were carried out following the National Institutes of Health guidelines for animal care and use. Animal protocols were approved by the Institutional Animal Care and Use Committee at Virginia Polytechnic Institute and State University. Female Balb/c mice (6-7 weeks of age, 16-20 g) were randomized into vaccine and control groups (8 per group). In the vaccine groups, mice were immunized subcutaneously with conjugate vaccine or nanovaccines containing 25 µg of Nic-KLH immunogen on days 0, 14, and 28. For groups immunized with vaccine and adjuvant, alum (1.5 mg) was pre-mixed with the vaccine solution before injection. Mice were injected with a total volume of 200 µL in all groups. In the blank group, 200 µL of PBS was injected into mice on the same days. Blood samples (~100 µL) were collected from the retro-orbital plexus of mice under isoflurane anesthesia on days 0, 13, 27, 41, 55, and 62 to monitor antibody titers.

Evaluation of the immunogenicity of nicotine vaccines by measuring specific anti-nicotine IgG antibody titers

Anti-nicotine IgG antibody titers in mouse serum samples were analyzed by an enzyme-linked immunosorbent assay (ELISA) according to a method reported previously.¹⁹ Antibody titer was defined as the dilution factor at which absorbance at 450 nm declined to half maximal.

Evaluation of the pharmacokinetic efficacy of nicotine vaccines in mice

Female Balb/c mice (6-7 weeks of age, 16-20 g) were immunized with 100 nm nanovaccine, 500 nm nanovaccine, or 6-CMUNic-KLH, and the negative control (KLH protein only), with or without the alum adjuvant using the same procedure described above (4 per group). For 6-CMUNic-KLH, two groups of mice were immunized using either 0.25 or 1.5 mg alum as adjuvant. Two weeks after the second boost injection (day 41), mice were administered 0.06 mg/kg nicotine subcutaneously. Mice were euthanized under anesthesia 4 min post nicotine challenge, and the blood and brain were collected. Nicotine contents in serum and brain tissues were analyzed by gas chromatography/mass spectrometry according to a method reported previously²⁴.

Statistical analyses

Data are expressed as means ± standard deviation. Comparisons among multiple groups were conducted using one-way ANOVA followed by Tukey's HSD test. The analysis of Th1/Th2 index between each vaccine treatment group and the value "1" was carried out by one-sample t-test. Differences were considered significant when the p-values were less than 0.05.

Results

Synthesis and characterization of lipid-polymeric hybrid NP-based nicotine vaccines with controlled size

Two hybrid NP-based nanovaccines with sizes of 100 and 500 nm were prepared, and their physiochemical properties were studied. As shown in Table 1, the sizes of lipid-polymeric hybrid and nanovaccine NPs were dominated by the size of the PLGA NPs. A slight increase of size was observed for the hybrid NPs and the final nanovaccine NPs compared to the initial PLGA NPs. Moreover, the size of the PLGA NPs can be controlled by changing the magnitude and time of sonication in the double emulsion solvent evaporation process. Therefore, hybrid NP-based nanovaccines with different sizes can be prepared reproducibly.

The measured mean diameters of the 100 and 500 nm nanovaccines were 108.7 ± 3.7 and 467.5 ± 10.3 nm, respectively (Table 1). This indicated that the fabrication method used in this study allowed accurate size control of the hybrid NP-based nanovaccines. The surface charges of nanovaccine NPs, represented by the zeta potential, were 2.29 ± 0.31 and 2.69 ± 0.07 mV for the 100 and 500 nm vaccines, respectively (Table 1). The polydispersity indexes (PDI) were 0.20 ± 0.02 and 0.23 ± 0.03 for the 100 and 500 nm nanovaccines, respectively (Table 1). The low PDI of the two nanovaccines indicated that the size of the NPs was uniform. In this study, 10 mg of KLH was used to associate with 50 mg of hybrid NPs. As shown in Table 1, the KLH conjugation efficiency was as high as 88% for both nanovaccines, demonstrating the high conjugation efficiency of the Traut's reagent- and maleimide-mediated reactions, as well as the high antigen loading capacity of hybrid NPs.

The morphology of hybrid NPs with distinct sizes was characterized by transmission electron microscopy (TEM). As shown in Figure 1A, hybrid 100 and 500 nm NPs clearly exhibited a core-shell hybrid structure. In the micro-images, the lipid shell is pinpointed by the blue arrows, and the PLGA core is shown by the red arrows. In agreement with the low PDI of NPs (Table 1), the particle sizes of both 100 and 500 nm NPs were uniform, suggesting that the NP fabrication method was highly effective and robust.

To confirm the hybridization of PLGA NPs and liposomes, Fourier transform infrared (FTIR) spectra of PLGA NPs, liposomes, and lipid-polymeric hybrid NPs were analyzed. As shown in Figure 1B, hybrid NPs shared unique wavelength peaks with either PLGA NPs or liposomes. For example, peaks at 1095 and 1136 cm^{-1} were shared by PLGA and hybrid NPs, while peaks at 2854 and 2925 cm^{-1} were commonly displayed in both liposomes and hybrid NPs. The similarities and differences in the FTIR spectra of hybrid NPs and the other two particles further suggested that a lipid layer was successfully coated onto PLGA NPs.

To verify the successful conjugation of KLH to hybrid NPs, NPs, in which KLH and the lipid layer were fluorescently labeled with rhodamine B and nitro-2-1,3-benzoxadiazol-4-yl (NBD), respectively, were imaged with confocal laser scanning microscopy (CLSM). Co-localization of both red and green color was observed on the majority of NPs, indicating that the maleimide-thiol reaction was highly efficient in conjugating protein to NPs (Figure 2). High conjugation efficiency between Nic-KLH and hybrid NPs is of great value to the vaccine design in this study. Firstly, it allows full utilization of both hybrid NPs and KLH,

avoiding laborious purification of unconjugated particles and proteins. Secondly, high quantities of KLH can be loaded onto a single NP, supplying sufficient amount of protein antigen to immune cells once internalized. Finally, high protein loading capacity can deliver more nicotine epitopes on a single NP, increasing the chance of B cell activation.

Uptake of hybrid NPs by dendritic cells

Efficient recognition and capture of antigens by antigen presenting cells largely determines the outcome of the humoral immune response. In this study, the influence of NP size on the uptake of nanovaccines by dendritic cells was investigated. Within 2 h, 99.4%-99.7% of the cells were stained by AF647 fluorescence. There was no marked difference in the percentages of positive dendritic cells for NPs of the two sizes (Figure 3C). This suggested that both 500 and 100 nm particles were taken up rapidly by dendritic cells. However, as shown in Figure 3D and 3E, a significantly higher mean intensity of AF647 fluorescence was observed in cells treated with 100 nm particles than in cells treated with 500 nm particles, demonstrating that dendritic cells can more efficiently swallow nanovaccine NPs of smaller size. Moreover, as shown in Figure 3A and 3B, the mean intensity of AF647 fluorescence in the 500 nm nanovaccine group was significantly higher than that in the AF647-KLH group, indicating that the use of hybrid NPs enhanced the bioavailability and internalization of protein antigens.

Cellular uptake of AF647- and NBD-labeled NPs was further studied using CLSM. As shown in Figure 4, the fluorescence intensity indicated that the amount of NPs taken up by dendritic cells was time-dependent for both NPs. In agreement with the flow cytometry results, all studied dendritic cells were stained by NPs, supporting the conclusion that both 500 and 100 nm NPs can be captured effectively by dendritic cells in a short period of time. Moreover, the brighter fluorescence of both AF647 and NBD in the 100 nm group (Figure 4A) compared to the 500 nm group (Figure 4B) at 2 h showed that more 100 nm NPs were internalized by dendritic cells. The amount of NPs carrying antigens that are internalized by dendritic cells is of great importance to activation of the immune response because the more antigen that is internalized, the more antigen peptides may be presented to naïve T cells, and the more B cells that may be activated.

Immunogenicity of hybrid NP-based nicotine nanovaccines in mice

A steady increase of the anti-nicotine antibody titer was observed for each vaccine after each injection (Figure 5). Specially, the anti-nicotine antibody titers increased significantly after the first booster injection (on day 27) for all vaccine groups. In addition, substantially increased antibody titers (>8,500) were detected for all formulations, except for the Nic-KLH conjugate vaccine, on day 41. Compared to the Nic-KLH conjugate vaccine, both the 100 and 500 nm nanovaccines achieved significantly higher anti-nicotine antibody titers on days 27, 41, 55, and 62. This demonstrated that the use of lipid-polymeric NPs as delivery vehicles could improve the immunogenicity of the Nic-KLH conjugate nicotine vaccine. Moreover, at the end of the immunogenicity study on day 62, the 100 nm nanovaccine without alum achieved significantly higher antibody titers over the 500 nm nanovaccine without alum; meanwhile, the 100 nm nanovaccine with alum also induced considerably

higher antibody titer than the 500 nm nanovaccine with alum. These results suggest that the 100 nm nanovaccine induced a stronger immunogenic effect.

In this study, 6-CMUNic-KLH, one of the most well-characterized and highly immunogenic conjugate nicotine vaccines²⁴, was used as a positive control. Among all formulations, the 100 nm nanovaccine with alum generated a much higher anti-nicotine antibody titer over 6-CMUNic-KLH at all studied time points. To study the long-term persistence of the immune response, antibody titers on days 55 and 62 were measured for all vaccine formulations. The antibody level in the 6-CMUNic-KLH group markedly declined from 11,000 to 8000 between days 41 and 55. Similarly, a pronounced decline of antibody titers was observed for nanovaccines with alum between days 55 and 62. Nevertheless, nanovaccines maintained antibody titers for a longer time compared to 6-CMUNic-KLH. Interestingly, antibody titers of nanovaccines without alum increased between days 55 and 62, especially for the 100 nm nanovaccine. This revealed that, at later times, the antibody titers in groups treated with nanovaccines without alum were higher and longer lasting than nanovaccines with alum. A possible mechanism of this finding is that alum limited the bioavailability of nanovaccines to immune cells, such as dendritic and B cells, due to the over-retention of NPs in alum²⁵.

The titers of IgG subclass antibodies, including IgG1, IgG2a, IgG2b, and IgG3 on day 62, were also measured. Nanovaccines, regardless of size, considerably increased the titers of all four IgG subclasses compared to the Nic-KLH conjugate vaccine, especially for IgG1 and IgG2a (Figure 6). Interestingly, the 100 nm nanovaccine group had significantly higher titers of IgG1 and IgG2a compared to the 500 nm nanovaccine group. In addition, as shown in Figure 6 and Table 2, IgG1 was dominant among all subclasses for all vaccines.

The Th1/Th2 index, that reflects the relative magnitude of the humoral to the cellular immune response²⁶, was calculated. Very low Th1/Th2 indexes (significantly less than 1) were found for all vaccine formulations and there were no significant differences among groups (Table 2). This indicated that the immune response induced by all tested nicotine vaccines was significantly skewed toward Th2. For nicotine vaccines, a low Th1/Th2 index is desirable because the efficacy of reducing the rewarding effects of nicotine is dependent on the magnitude of the humoral response.

Effects of nicotine nanovaccines on the distribution of nicotine in serum and brain

The ability of vaccines to prevent nicotine from crossing the blood-brain barrier largely determines the outcomes of smoking cessation efforts.⁷ To determine the efficacy of nicotine nanovaccines, mice were challenged with 0.06 mg/kg nicotine two weeks after the second boost immunization (on Day 41) and nicotine contents in serum and brain were analyzed. This dose approximates the mg/kg of nicotine in three smoked cigarettes in humans²⁷. The nicotine contents retained in serum are shown in Figure 7A. The serum nicotine level increased by 47% in the 500 nm nanovaccine group compared to that of the negative control group. In contrast, serum nicotine levels increased by 119 and 407% in the 100 nm nanovaccine group without or with 1.5 mg of alum, respectively. This suggested that the 100 nm nanovaccine had a better efficacy on retaining nicotine in serum. Remarkably, the serum nicotine level in the 500 nm nanovaccine with alum group was lower than that in the negative controls, although the nicotine antibody titer was fairly high (Figure 5).

Figure 7B shows the nicotine contents distributed into brain. Significant reductions of brain nicotine levels were observed in all nanovaccine groups compared to the negative control group. Compared to the negative control group, brain nicotine levels were reduced by 32.0, 56.2, 39.5, and 41.7% in the 100 nm nanovaccine, 100 nm with alum nanovaccine, 500 nm nanovaccine, and 500 nm with alum nanovaccine groups, respectively. Although efficacy was not improved in the 100 nm without alum nanovaccine versus the 500 nm without alum nanovaccine group, the 100 nm with alum nanovaccine group achieved 15% more brain nicotine reduction compared to the 500 nm with alum nanovaccine group. The 100 nm nanovaccine appeared to have a better PK efficacy than the 500 nm nanovaccine in the presence of the alum adjuvant, which was reflected by its lower mean nicotine level in the brain of mice.

Due to its poor anti-nicotine antibody producing activity, Nic-KLH was not used in this PK study. Instead, we compared the PK results of nanovaccines to that of a positive control using 6-CMUNic-KLH that blocked up to 80% of nicotine from entering into the brain of rats.^{12, 28} The 100 nm without alum and 500 nm without alum nanovaccine groups had comparable average brain nicotine levels compared to the 6-CMUNic-KLH with 0.25 mg of alum group. In addition, the brain nicotine level in the 100 nm with alum group, in which 1.5 mg of alum was used, was also comparable to that in the 6-CMUNic-KLH with 1.5 mg of alum group. In this study, we determined the antibody titer but did not test the specificity of antibodies, because the PK study provided the ultimate evaluation of vaccine efficacy.

Evaluation of the safety of hybrid NP-based nicotine nanovaccines in mice

The safety of nanovaccines was investigated histopathologically. There were no lesions in the hearts, lungs, livers, spleens, and kidneys of mice treated with nanovaccines with or without alum (Figure 8A). This demonstrated that the hybrid NP-based nicotine nanovaccine did not cause detectable lesions to organs and thus appeared to be safe. In addition, as shown in Figure 8B, no changes of body weights were found during the entire study period in all of the mice treated with various nicotine vaccines, nor were the body weights different from the PBS control. These results also suggest that the nanovaccine is safe.

Discussion

Vaccines are a promising approach to treat nicotine addiction by inducing the production of nicotine-specific antibodies that can bind with nicotine in blood fluid and thus block it from entering the brain where nicotine would stimulate the central nervous system to generate euphoria and thereby cause nicotine addiction.⁸ Unfortunately, to date, all clinically tested hapten-protein conjugate nicotine vaccines have failed due to their poor ability to generate a sufficient anti-nicotine antibody titer. This failure can be attributed to their intrinsic shortfalls including poor recognition and internalization of nicotine by immune cells, low bioavailability, and fast degradation.^{7, 29} In this study, for the first time, we report the development of a lipid-polymeric hybrid NP-based nicotine vaccine. We used hybrid NPs as a means for efficient delivery of conjugate nicotine vaccines to address the limitations mentioned above and to improve the immunogenicity of the vaccine. In addition, we studied

the influence of particle size on the efficacy of nanovaccines and illustrated the necessity of controlling the particle size in maximizing the immunogenicity of the nanovaccine.

The nanovaccine studied here was designed to have multiple Nic-KLH conjugates attached on the surface of lipid-polymeric hybrid NPs. TEM results indicated that a core-shell hybrid structure was formed for hybrid NPs of both 100 and 500 nm. The hybrid structure was important to the immunological outcome of the nanovaccines. The particulate nature of PLGA NPs offers extra rigidity to liposomes, enhancing their stability and lengthening their circulation time.^{30, 31} The lipid membrane surface of hybrid NPs may also improve particle internalization by immune cells through membrane fusion.³² In addition, the lipid shell may act as a shield between the aqueous surroundings and the PLGA core, providing protection to PLGA NPs from hydrolytic degradation as well as contributing to long-term stability of the hybrid structure³³.

Due to its many advantages, such as high immunogenicity and clinically proven safety, KLH has been used widely as a carrier protein for vaccine development.³⁴ In the vaccine design of this study, KLH functioned as a support for the nicotine hapten as well as a potent stimulator of T helper cells. CLSM and protein assay results demonstrated that the Nic-KLH antigen was attached to hybrid NPs at high conjugation and loading efficiencies. This may not only have supplied sufficient amounts of protein antigen to immune cells to generate enough T helper cells once NPs were internalized, but also provided sufficient nicotine epitopes on a single NP to increase the chance of B cell recognition and activation.

Zeta-potential results revealed that both 100 and 500 nm nanovaccines were positively charged due to the inclusion of a cationic lipid (1,2-dioleoyl-3-trimethylammonium-propane) in the lipid formulation. Because the membranes of immune cells are composed largely of negatively charged phospholipids, the positive surface charge of nanovaccine NPs can enhance their interaction with immune cells, thereby promoting cellular uptake of the nanovaccine.³⁵ All of these hybrid NP-based nanovaccine properties can potentially enhance the vaccine's immunogenic efficacy.

In vitro cellular uptake data revealed that the internalization of Nic-KLH conjugate antigens was enhanced significantly by the utilization of hybrid NPs as a delivery vehicle. This enhanced internalization may be caused by the increased availability of antigens for uptake following the conjugation of multiple Nic-KLH antigens to one NP. In addition, the optimal physicochemical properties mentioned above may contribute to the improved internalization process. Moreover, 100 nm nanovaccine particles were taken up by dendritic cells more efficiently than 500 nm particles. The enhanced internalization of antigens could lead to a stronger immune response. In agreement with the *in vitro* data, *in vivo* immunization data demonstrated that the use of hybrid NPs, regardless of size, could significantly enhance the immunogenicity of Nic-KLH conjugate vaccines.

As mentioned above, traditional conjugate nicotine vaccines that have been evaluated in clinical trials are ineffective due to their limited immunogenicity.⁷ The findings presented here are thus of great value in providing a novel strategy to improve the immunogenicity of conjugate nicotine vaccines. Both the ELISA and PK study results revealed that the 100 nm

nanovaccine resulted in better immunogenicity and PK efficacy than the 500 nm nanovaccine, especially in the presence of alum. This finding suggested another potential approach to improve the efficacy of NP-based nicotine vaccines. The 6-CMUNic-KLH conjugate vaccine, which is one of the most well-characterized and highly immunogenic conjugate nicotine vaccines²⁴, was used as a positive control in this study. 6-CMUNic-KLH exhibited substantial potency in eliciting nicotine antibodies, resulting in excellent PK efficacy in preclinical studies. Previous studies showed that 6-CMUNic-KLH induced an anti-nicotine antibody titer up to 200,000 and blocked up to 80% of nicotine from entering into the brain of rats.^{12, 28, 36} In the current study, the 100 nm nanovaccine administered with alum resulted in a considerably higher anti-nicotine antibody titer and a comparable efficacy of reducing brain nicotine levels, compared to 6-CMUNic-KLH. The 6-CMUNic-KLH used in this study was an optimized formulation. However, the lipid-polymeric NP-based nicotine nanovaccines used in this study were not optimized by strategies other than modulating the particle size. It is very possible that the efficacy of hybrid NP-based nicotine vaccines would be further improved after optimization via multiple strategies, such as modulating the hapten density, selection of carrier proteins, and use of molecular adjuvants.

Overall, the hybrid NP-based nicotine nanovaccines used in this study were safe in mice. All data suggest that the lipid-polymeric NP-based nicotine vaccine is a promising candidate to treat nicotine addiction. The immunogenicity of conjugate nicotine vaccine can be improved by the use of lipid-polymeric hybrid NPs, suggesting a new strategy to enhance the efficacy of conjugate nicotine vaccines. The immunogenicity and PK efficacy of the hybrid NP-based nicotine nanovaccine can be enhanced by modulating the particle size. This approach can potentially be applied in the development of other drug abuse and NP-based vaccines.

Supplementary Material

Refer to Web version on PubMed Central for supplementary material.

Acknowledgments

We thank the Morphology Lab at Virginia Tech University for their assistance with the TEM imaging. We also thank the Fralin Confocal Lab for assistance with the CLSM imaging.

Funding: This work was financially supported by the National Institute of Health (National Institute on Drug Abuse) through grant number U01DA036850.

References

1. Xue S, Schlosburg JE, Janda KD. A new strategy for smoking cessation: Characterization of a bacterial enzyme for the degradation of nicotine. *J Am Chem Soc.* 2015; 137:10136–9. [PubMed: 26237398]
2. Benowitz NL. Nicotine addiction. *N Engl J Med.* 2010; 362:2295–303. [PubMed: 20554984]
3. Chen LS, Baker TB, Jorenby D, Piper M, Saccone N, Johnson E, et al. Genetic variation (CHRNA5), medication (combination nicotine replacement therapy vs varenicline), and smoking cessation. *Drug Alcohol Depend.* 2015; 154:278–82. [PubMed: 26142345]
4. Jain R, Majumder P, Gupta T. Pharmacological intervention of nicotine dependence. *BioMed Res Int.* 2013; 2013

5. Carpenter MJ, Jardin BF, Burriss JL, Mathew AR, Schnoll RA, Rigotti NA, et al. Clinical strategies to enhance the efficacy of nicotine replacement therapy for smoking cessation: A review of the literature. *Drugs*. 2013; 73:407–26. [PubMed: 23572407]
6. Raupach T, Hoogsteder PH, Onno van Schayck CP. Nicotine vaccines to assist with smoking cessation: current status of research. *Drugs*. 2012; 72:e1–16.
7. Pentel PR, LeSage MG. New Directions in nicotine vaccine design and use. *Adv Pharmacol*. 2014; 69:553–80. [PubMed: 24484987]
8. LeSage MG, Keyler DE, Pentel PR. Current status of immunologic approaches to treating tobacco dependence: Vaccines and nicotine-specific antibodies. *Aaps J*. 2006; 8:E65–E75. [PubMed: 16584135]
9. Syed BA, Chaudhari K. Smoking cessation drugs market. *Nat Rev Drug Discov*. 2013; 12:97–8. [PubMed: 23370239]
10. Hatsukami DK, Jorenby DE, Gonzales D, Rigotti NA, Glover ED, Oncken CA, et al. Immunogenicity and smoking-cessation outcomes for a novel nicotine immunotherapeutic. *Clin Pharmacol Ther*. 2011; 89:392–9. [PubMed: 21270788]
11. Cornuz J, Zwahlen S, Jungi WF, Osterwalder J, Klingler K, van Melle G, et al. A vaccine against nicotine for smoking cessation: A randomized controlled trial. *Plos One*. 2008; 3:e2547. [PubMed: 18575629]
12. Keyler DE, Roiko SA, Earley CA, Murtaugh MP, Pentel PR. Enhanced immunogenicity of a bivalent nicotine vaccine. *Int Immunopharmacol*. 2008; 8:1589–94. [PubMed: 18656557]
13. Song W, Tang Z, Lei T, Wen X, Wang G, Zhang D, et al. Stable loading and delivery of disulfiram with mPEG-PLGA/PCL mixed nanoparticles for tumor therapy. *Nanomedicine*. 2016; 12:377–86. [PubMed: 26711966]
14. Doll TAPF, Neef T, Duong N, Lanar DE, Ringler P, Muller SA, et al. Optimizing the design of protein nanoparticles as carriers for vaccine applications. *Nanomed-Nanotechnol*. 2015; 11:1705–13.
15. Gebril AM, Lamprou DA, Alsaadi MM, Stimson WH, Mullen AB, Ferro VA. Assessment of the antigen-specific antibody response induced by mucosal administration of a GnRH conjugate entrapped in lipid nanoparticles. *Nanomed-Nanotechnol*. 2014; 10:971–9.
16. Dasgupta Q, Madras G, Chatterjee K. Controlled release kinetics of p-aminosalicylic acid from biodegradable crosslinked polyesters for enhanced anti-mycobacterial activity. *Acta Biomater*. 2016; 30:168–76. [PubMed: 26596566]
17. Adams JR, Haughney SL, Mallapragada SK. Effective polymer adjuvants for sustained delivery of protein subunit vaccines. *Acta Biomater*. 2015; 14:104–14. [PubMed: 25484331]
18. Lockner JW, Ho SO, McCague KC, Chiang SM, Do TQ, Fujii G, et al. Enhancing nicotine vaccine immunogenicity with liposomes. *Bioorg Med Chem Lett*. 2013; 23:975–8. [PubMed: 23313243]
19. Hu Y, Zheng H, Huang W, Zhang CM. A novel and efficient nicotine vaccine using nano-lipoplex as a delivery vehicle. *Hum Vacc Immunother*. 2014; 10:64–72.
20. Zheng H, Hu Y, Huang W, de Villiers S, Pentel P, Zhang JF, et al. Negatively charged carbon nanohorn supported cationic liposome nanoparticles: A novel delivery vehicle for anti-nicotine vaccine. *J Biomed Nanotechnol*. 2015; 11:2197–210. [PubMed: 26510313]
21. Hu Y, Hoerle R, Ehrich M, Zhang CM. Engineering the lipid layer of lipid-PLGA hybrid nanoparticles for enhanced in vitro cellular uptake and improved stability. *Acta Biomater*. 2015; 28:149–59. [PubMed: 26428192]
22. Chua BY, Sekiya T, Al Kobaisi M, Short KR, Mainwaring DE, Jackson DC. A single dose biodegradable vaccine depot that induces persistently high levels of antibody over a year. *Biomaterials*. 2015; 53:50–7. [PubMed: 25890706]
23. Rosalia RA, Cruz LJ, van Duikeren S, Tromp AT, Silva AL, Jiskoot W, et al. CD40-targeted dendritic cell delivery of PLGA-nanoparticle vaccines induce potent anti-tumor responses. *Biomaterials*. 2015; 40:88–97. [PubMed: 25465442]
24. de Villiers SHL, Cornish KE, Troska AJ, Pravetoni M, Pentel PR. Increased efficacy of a trivalent nicotine vaccine compared to a dose-matched monovalent vaccine when formulated with alum. *Vaccine*. 2013; 31:6185–93. [PubMed: 24176492]

25. Noe SM, Green MA, HogenEsch H, Hem SL. Mechanism of immunopotentiality by aluminum-containing adjuvants elucidated by the relationship between antigen retention at the inoculation site and the immune response. *Vaccine*. 2010; 28:3588–94. [PubMed: 20211692]
26. Moser M, Murphy KM. Dendritic cell regulation of TH1-TH2 development. *Nat Immunol*. 2000; 1:199–205. [PubMed: 10973276]
27. McCluskie MJ, Thorn J, Mehelic PR, Kolhe P, Bhattacharya K, Finneman JI, et al. Molecular attributes of conjugate antigen influence function of antibodies induced by anti-nicotine vaccine in mice and non-human primates. *Int Immunopharmacol*. 2015; 25:518–27. [PubMed: 25737198]
28. Pravetoni M, Keyler DE, Pidaparathi RR, Carroll FI, Runyon SP, Murtaugh MP, et al. Structurally distinct nicotine immunogens elicit antibodies with non-overlapping specificities. *Biochem Pharmacol*. 2012; 83:543–50. [PubMed: 22100986]
29. Shen XY, Orson FM, Kosten TR. Vaccines against drug abuse. *Clin Pharmacol Ther*. 2012; 91:60–70. [PubMed: 22130115]
30. Hu Y, Ehrich M, Fuhrman K, Zhang CM. In vitro performance of lipid-PLGA hybrid nanoparticles as an antigen delivery system: lipid composition matters. *Nanoscale Res Lett*. 2014; 9:434. [PubMed: 25232295]
31. Zhang LF, Granick S. How to stabilize phospholipid liposomes (using nanoparticles). *Nano Lett*. 2006; 6:694–8. [PubMed: 16608266]
32. Le Meins JF, Schatz C, Lecommandoux S, Sandre O. Hybrid polymer/lipid vesicles: state of the art and future perspectives. *Mater Today*. 2014; 17:92–3.
33. Cheow WS, Hadinoto K. Factors affecting drug encapsulation and stability of lipid-polymer hybrid nanoparticles. *Colloid Surface B*. 2011; 85:214–20.
34. Harris JR, Markl J. Keyhole limpet hemocyanin (KLH): a biomedical review. *Micron*. 1999; 30:597–623. [PubMed: 10544506]
35. Foged C, Brodin B, Frøkjær S, Sundblad A. Particle size and surface charge affect particle uptake by human dendritic cells in an in vitro model. *Int J Pharm*. 2005; 298:315–22. [PubMed: 15961266]
36. Hieda Y, Keyler DE, VandeVoort JT, Kane JK, Ross CA, Raphael DE, et al. Active immunization alters the plasma nicotine concentration in rats. *J Pharmacol Exp Ther*. 1997; 283:1076–81. [PubMed: 9399979]

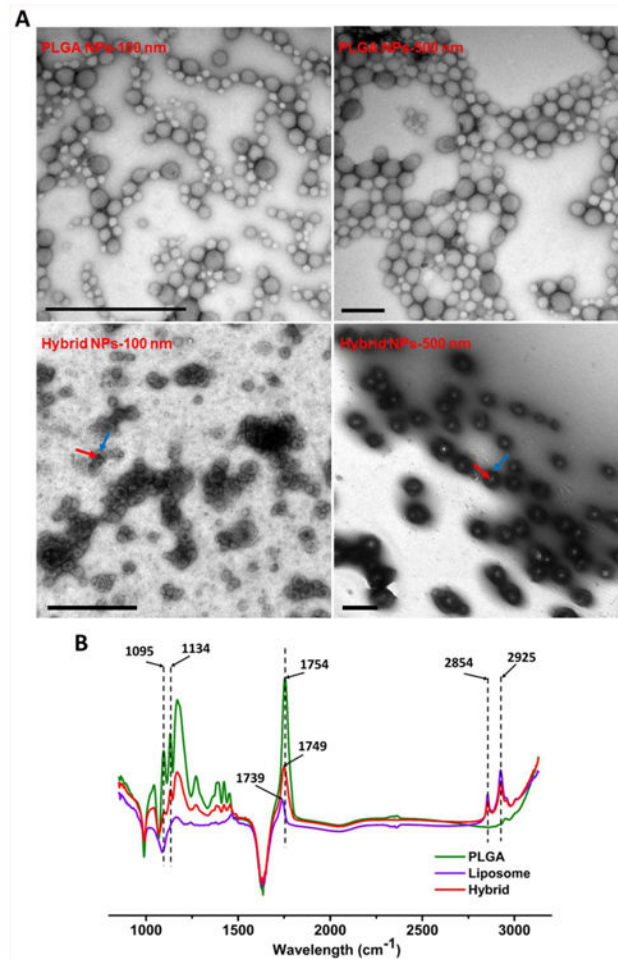


Figure 1. Characterization of lipid-polymeric hybrid NPs with different sizes. (A) Transmission electron microscopic images of poly(lactic-co-glycolic acid) (PLGA) and hybrid NPs with different average sizes. The red and blue arrows denote the PLGA core and lipid shell, respectively. The scale bars represent 1000 nm. (B) Fourier transform infrared spectra of PLGA NPs, liposome NPs, and lipid-polymeric hybrid NPs.

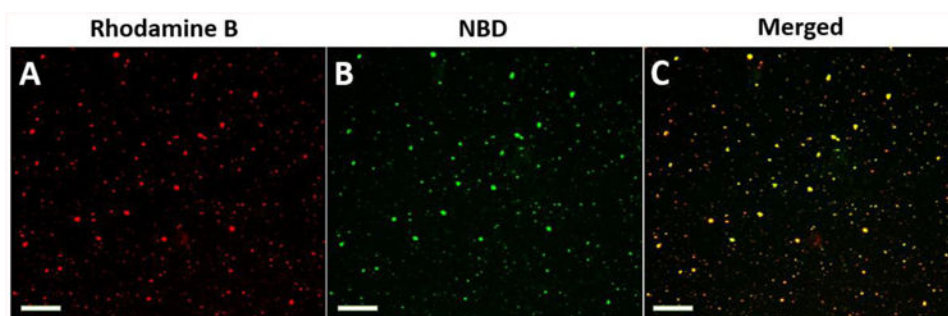


Figure 2. Confocal laser scanning microscopy images of KLH-conjugated lipid-polymeric hybrid NPs. KLH and lipids were labeled by (A) rhodamine B (red) and (B) NBD (green), respectively. (C) Dual labeling is shown in yellow. The scale bars represent 10 μm .

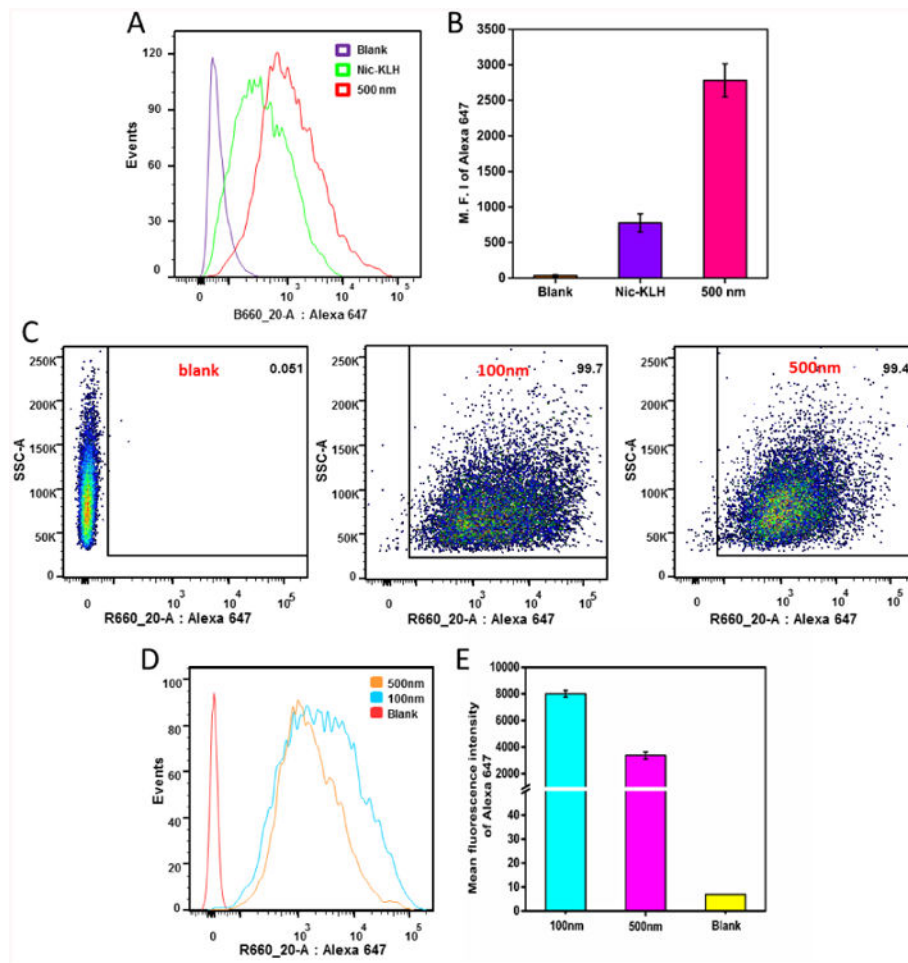


Figure 3.

Flow cytometry analysis of JAWSII dendritic cells treated with the AF647-KLH conjugate or AF647-labeled nanovaccine NPs of different sizes for 2 h. (A), (D) and (B), (E) show the intensity distribution and mean intensity of AF647 fluorescence, respectively, in dendritic cells treated with AF647-KLH or AF647-labeled nanovaccines. (C) Recorded events show that more than 99% of cells were labeled for both 100 and 500 nm nanovaccine particles. AF647 was conjugated to KLH to form the AF647-KLH conjugate. AF647-KLH was associated to the surface of hybrid NPs to form fluorescent nanovaccine NPs. The blank group are cells that were not treated with NPs. Quantitative data are expressed as means \pm SD.

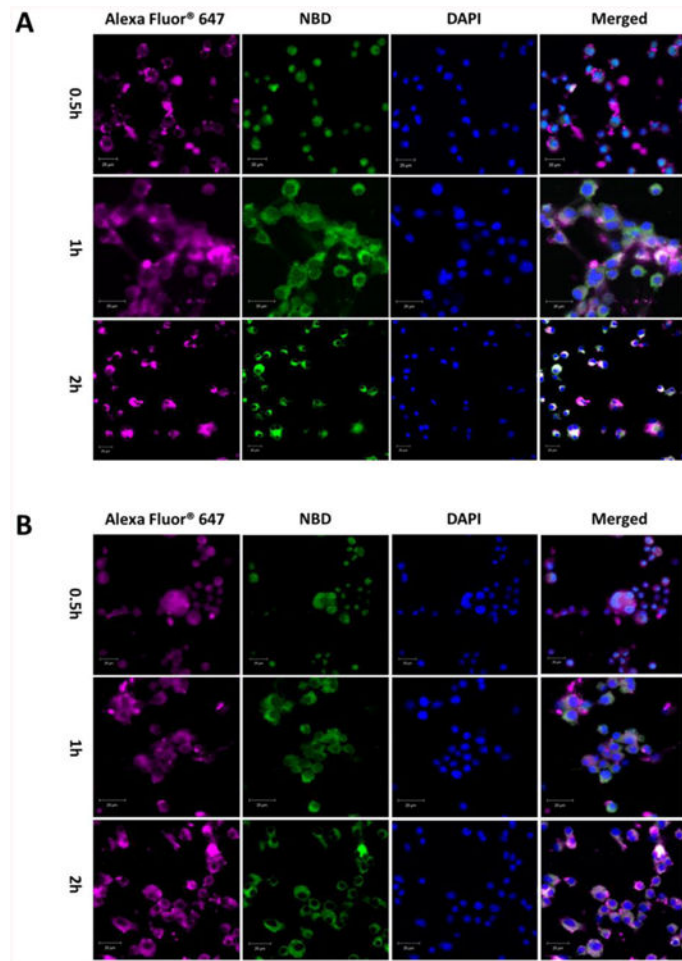


Figure 4. Confocal laser scanning microscopy images of JAWSII dendritic cells treated with (A) 100 nm or (B) 500 nm nanovaccine NPs for 0.5, 1, and 2 h. KLH was labeled with AF647 and the lipid layer of NPs was labeled with NBD. The scale bars represent 20 μm.

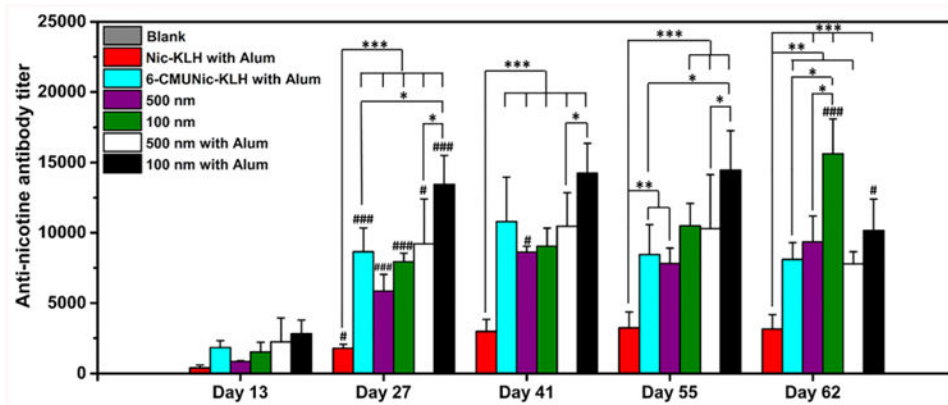


Figure 5. Time course of anti-nicotine-specific antibody formation in mice immunized with various nicotine vaccines. Mice (n = 8 per group) were immunized by subcutaneous injection on days 0, 14, and 28. In the blank group, mice were injected with phosphate-buffered saline as the negative control. Antibody titers were compared among groups using one-way ANOVA followed by Tukey's HSD test. Data are expressed as means ± SD. Significantly different antibody titers: *p < 0.05, **p < 0.01, ***p < 0.001. Antibody titers were significantly different compared to that of the previous study time point: # < 0.05, ### < 0.001.

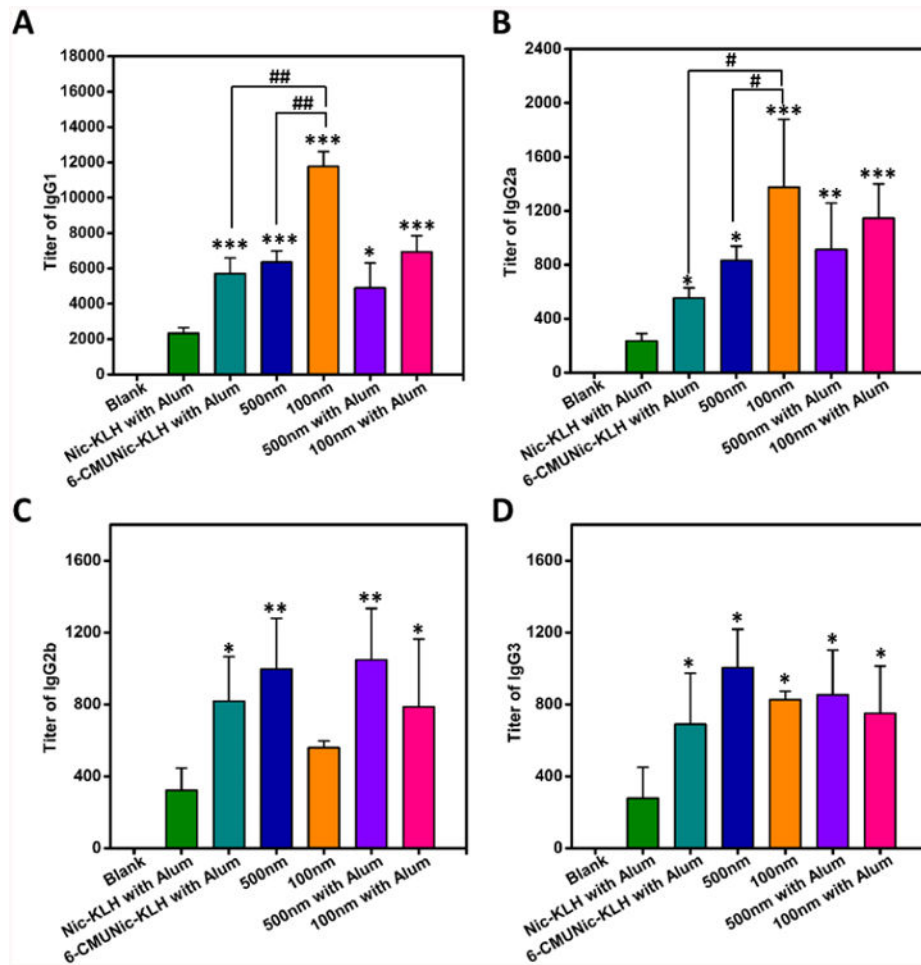


Figure 6. Distribution of IgG subclasses generated by immunization with nicotine vaccines. (A) IgG1; (B) IgG2a; (C) IgG2b; (D) IgG3. In the blank group, mice were injected with phosphate-buffered saline as the negative control. Comparisons among groups were analyzed by one-way ANOVA followed by Tukey's HSD test. Data are expressed as means \pm SD. Significantly different compared to the Nic-KLH with alum groups: * $p < 0.05$, ** $p < 0.01$, *** $p < 0.001$. Significantly different: # $p < 0.05$, ## $p < 0.01$.

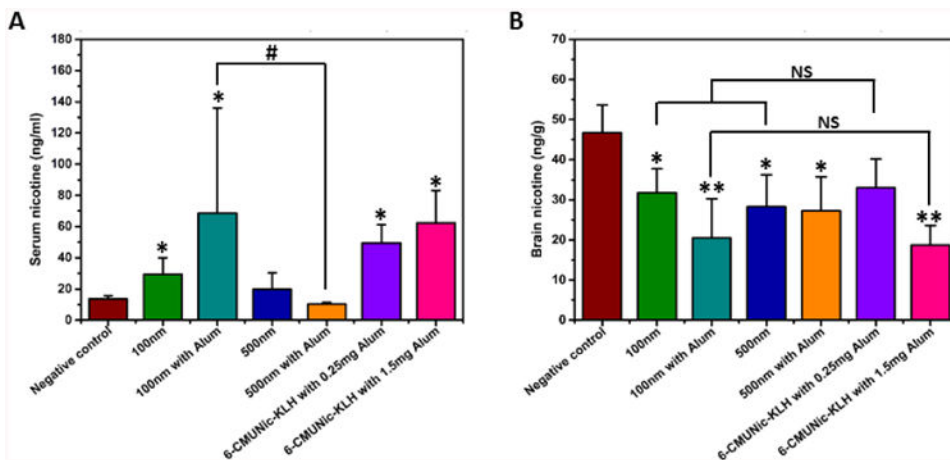


Figure 7. Nicotine distribution in serum and brain in immunized mice. Mice were immunized with vaccines containing immunogens equivalent to 25 μ g of Nic-KLH. For groups with alum, 1.5 mg was used as an adjuvant. The 6-CMUNic-KLH positive control used 0.25 or 1.5 mg of alum. Mice in the negative control group were immunized with 25 μ g of KLH carrier protein alone. (A) Serum and (B) brain tissues of 4 mice were collected 4 min post administration of 0.06 mg/kg nicotine subcutaneously on Day 41. Data are expressed as means \pm SD. Significantly different compared to the negative control group: *p < 0.05, **p < 0.01. Significantly different: #p < 0.05. NS indicates the brain nicotine levels between groups were comparable (p>0.98).

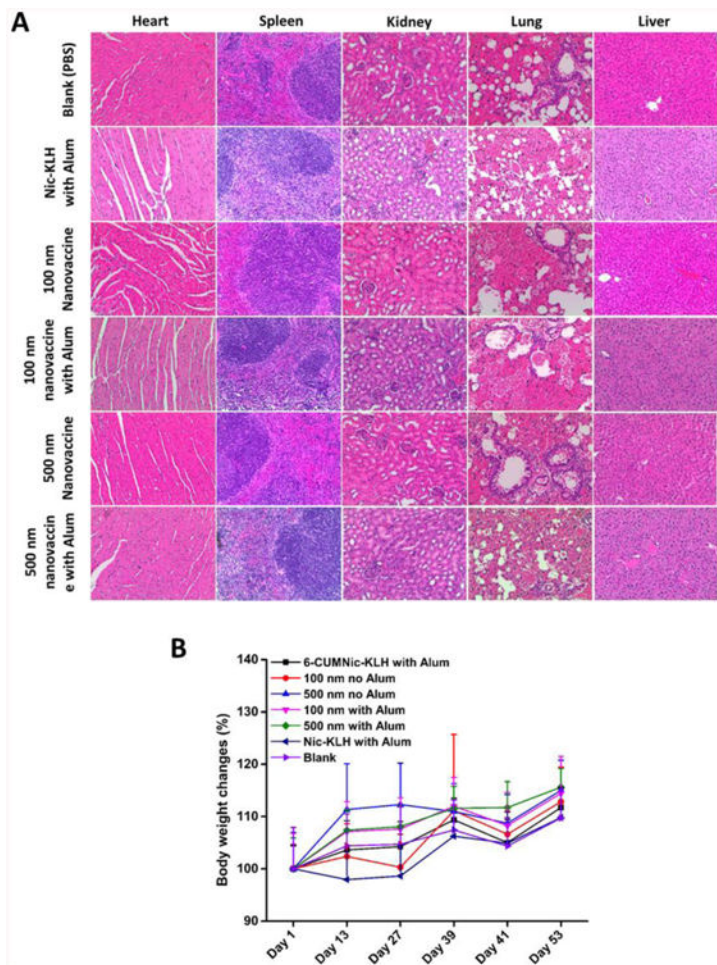


Figure 8. Evaluation of the safety of nicotine vaccines. (A) Representative histopathological images of tissues from mice treated nicotine vaccines. No lesions were observed in heart, kidney, liver, spleen, and lung tissues. (B) Body weight changes of immunized mice. Data are expressed as means \pm SD. No significant differences were found between mice treated with different vaccines and those treated with phosphate-buffered saline (blank).

Table 1

Physicochemical properties of NPs.

NPs	Size (d, nm)	Zeta potential (mV)	PDI	Nic-KLH conjugation efficiency (%)
PLGA NP-100 nm	98.5 ± 7.2	-4.32 ± 0.24	0.23 ± 0.03	--
PLGA NP-500 nm	451.6 ± 14.0	-4.94 ± 0.34	0.24 ± 0.03	--
Liposome	110.7 ± 4.5	10.70 ± 0.78	0.19 ± 0.02	--
Hybrid NP-100 nm	102.1 ± 4.5	9.60 ± 0.47	0.21 ± 0.03	--
Hybrid NP-500 nm	456.9 ± 7.8	10.10 ± 0.58	0.22 ± 0.04	--
Nanovaccine-100 nm	108.7 ± 3.7	2.29 ± 0.31	0.20 ± 0.02	88.28 ± 0.49
Nanovaccine-500 nm	467.5 ± 10.3	2.69 ± 0.07	0.23 ± 0.03	88.53 ± 2.02

Table 2

Th1/Th2 index of nicotine vaccines.

	100 nm	500 nm	6-CMUNic-KLH with Alum	100 nm with Alum	500 nm with Alum	Nic-KLH with Alum
IgG1 (%)	80.9	69.2	73.4	72.1	63.5	73.7
Th1/Th2 index	0.0935 ± 0.0359 ***	0.1444 ± 0.0214 ***	0.1090 ± 0.0240 ***	0.1368 ± 0.0303 ***	0.1800 ± 0.0457 ***	0.1098 ± 0.0479 ***

*** indicates the comparison between the Th1/Th2 indexes from each vaccine treatment group and the value "1", in which p-value is less than 0.001. No significant differences were found among the Th1/Th2 indexes with the different vaccine groups.